Supplementary Information

Identifying Multicellular Spatiotemporal Organization of Cells with SpaceFlow

Honglei Ren[1], Benjamin L. Walker[1,2], Zixuan Cang[3], Qing Nie[1,2,4,*]

[1] The NSF-Simons Center for Multiscale Cell Fate Research, University of California Irvine, Irvine, CA, 92627, USA

[2] Department of Mathematics, University of California Irvine, Irvine, CA, 92627, USA

[3] Department of Mathematics, North Carolina State University, Raleigh, NC 27695.

[4] Department of Developmental and Cell Biology, University of California Irvine, Irvine, CA, 92627, USA

[*] Corresponding Author: qnie@uci.edu

This file includes the following subsections:

- Supplementary Figures
- Supplementary Tables

Supplementary Figures

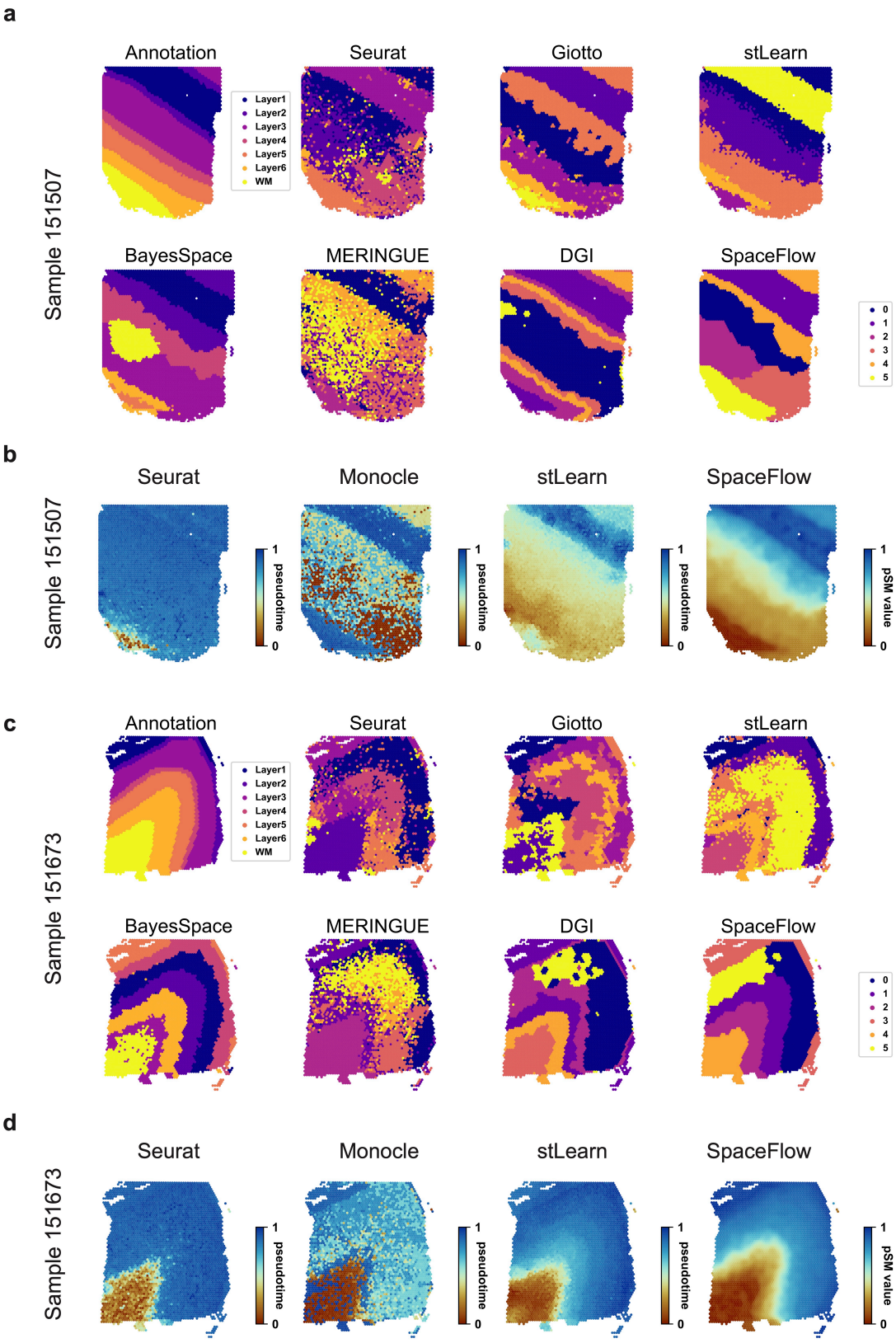

Supplementary Figure 1. Benchmarking on sections 151507 and 151673 using LIBD human dorsolateral prefrontal cortex (DLPFC) ST data [1]**. a**. Domain annotation (top left panel) and segmentations given by different methods (other panels) using section 151507 of DLPFC data. **b**. The spatial visualization of pseudotimes calculated by Seurat, Monocle, stLearn, and the pseudo-Spatiotemporal Map (pSM) generated by SpaceFlow on section 151507 of DLPFC data. **c.** Domain annotation (top left panel) and segmentations given by different methods (other panels) using section 151673 of DLPFC data. **d.** The spatial visualization of pseudotimes calculated by Seurat, Monocle, stLearn, and the pSM generated by SpaceFlow on section 151673 of DLPFC data.

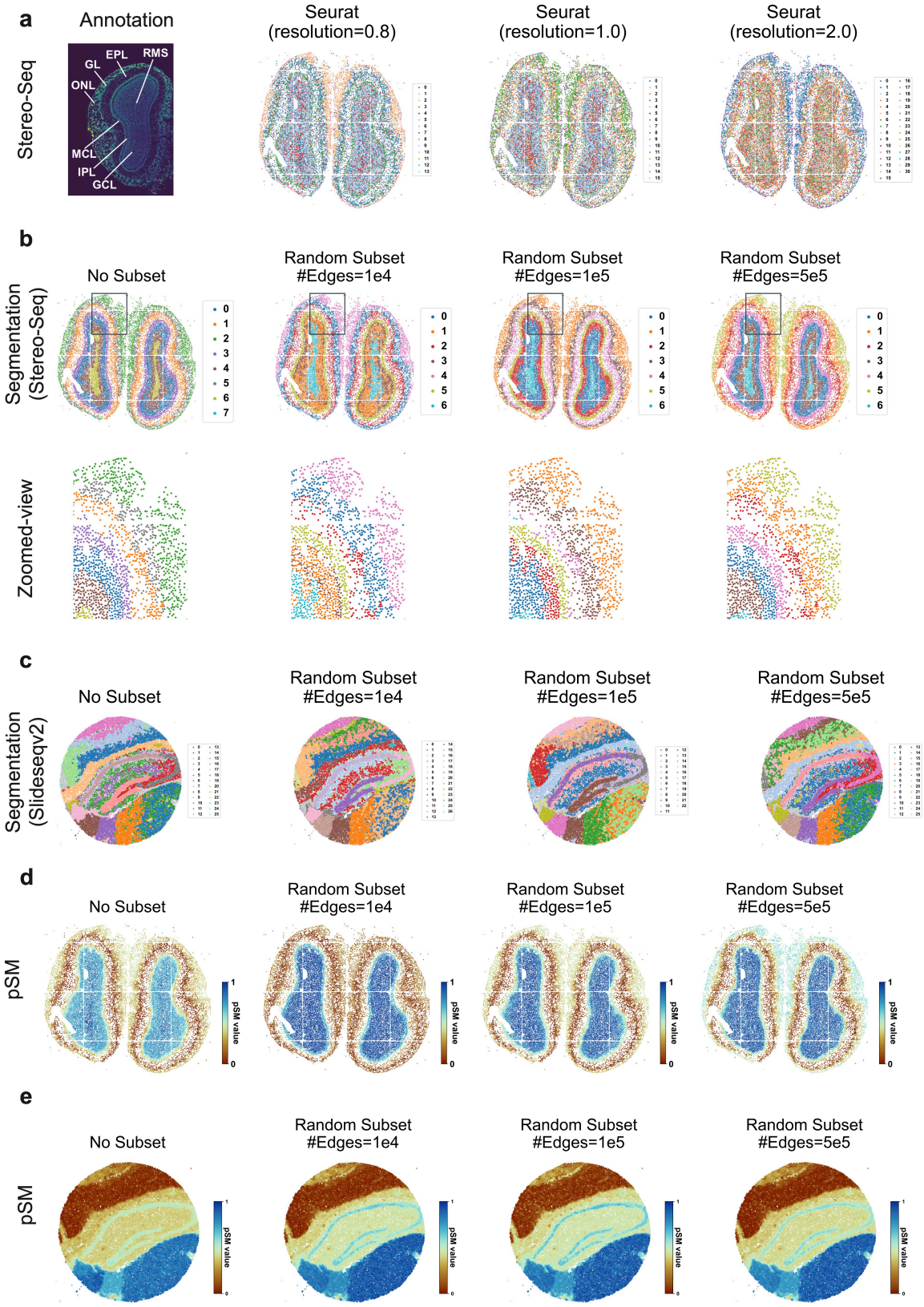
a
Annotation
Seurat (resolution=0.8)
Seurat (resolution=1.0)
Seurat (resolution=2.0)
Stereo-Seq
EPL
RMS
GL
ONL
MCL
IPL
GCL
b
No Subset
Random Subset #Edges=1e4
Random Subset #Edges=1e5
Random Subset #Edges=5e5
Segmentation (Stereo-Seq)
Zoomed-view
c
Segmentation (Slideseqv2)
d
pSM
pSM value
e

Supplementary Figure 2. Domain segmentation and pSM on Stereo-seq data and Slide-seqv2 data. a. Domain annotation (left panel) and segmentations given by Seurat with different resolution settings (right three panels) on Stereo-seq data. **b-c**. Domain segmentations of (**b**) Stereo-seq data and (**c**) Slide-seqv2 data given by SpaceFlow computing regularization over different subsets of cells, showing lack of meaningful variation even when regularization is computed over only a subset. **d-e.** The pseudo-Spatiotemporal Map (pSM) of (**d**) Stereo-seq data and (**e**) Slide-seqv2 data given by SpaceFlow computing regularization over different subsets of cells, again showing qualitatively matching results in each case.

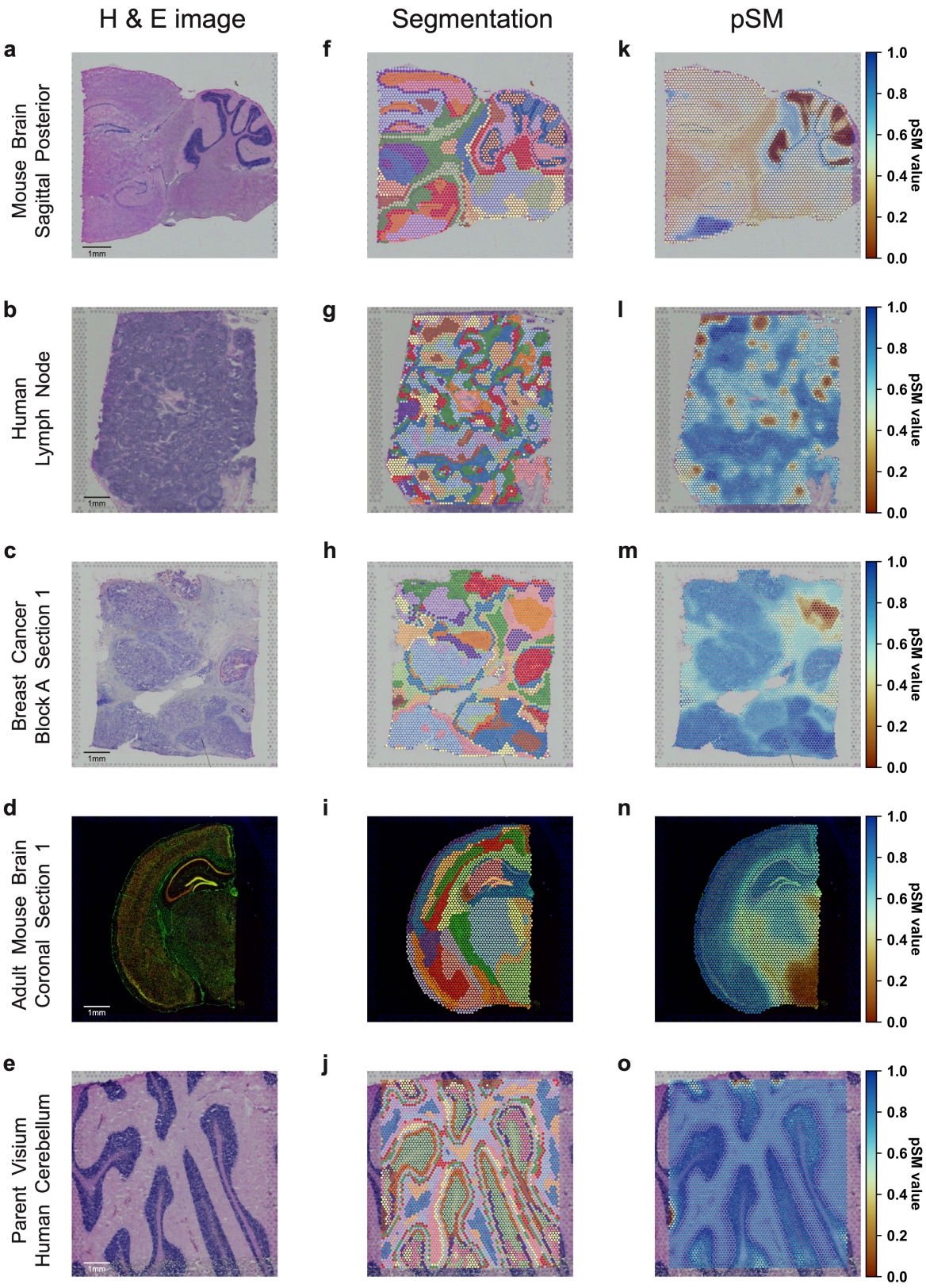
H & E image
Segmentation
pSM
a
Mouse Brain
Sagittal Posterior
b
Human
Lymph Node
c
Breast Cancer
Block A Section 1
d
Adult Mouse Brain
Coronal Section 1
e
Parent Visium
Human Cerebellum
f
g
h
i
j
k
l
m
n
o
1mm
pSM value
1.0
0.8
0.6
0.4
0.2
0.0

Supplementary Figure 3. Domain segmentation and pSM on five 10x Genomics official Visium datasets. a-e. H & E images of five Visium datasets (**a**. V1 Mouse Brain Sagittal Posterior, **b**. V1 Human Lymph Node, **c**. V1 Breast Cancer Block A Section 1, **d**. V1 Adult Mouse Brain Coronal Section 1, **e**. Parent Visium Human Cerebellum). **f-j.** Domain segmentations of the corresponding datasets given by SpaceFlow. **k-o**. pSM of the five datasets given by SpaceFlow.

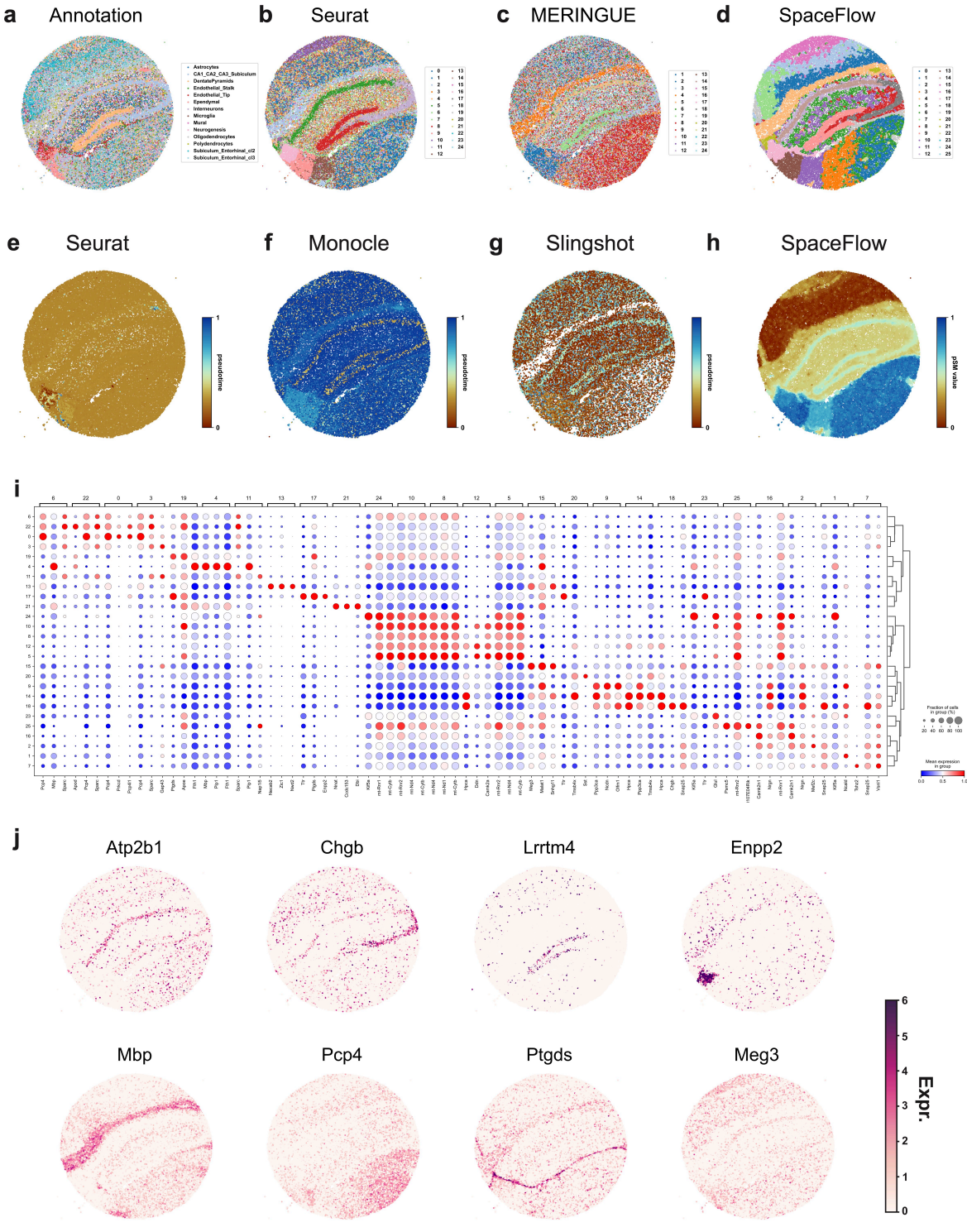
a
Annotation
b
Seurat
c
MERINGUE
d
SpaceFlow
e
Seurat
f
Monocle
g
Slingshot
h
SpaceFlow
pseudotime
pseudotime
pseudotime
pSM value
i
j
Atp2b1
Chgb
Lrrtm4
Enpp2
Mbp
Pcp4
Ptgds
Meg3
Expr.

Supplementary Figure 4. SpaceFlow analysis on slideseq v2 dataset [2]**. a-** Annotation **b-d**. Domain segmentations produced by Seurat (**b**), MERINGUE (**c**) and SpaceFlow (**d**). **e-h**. The spatial visualization of pseudotimes calculated by Seurat (**e**), Monocle (**f**), Slingshot (**g**), and the pSM generated by SpaceFlow (**h**). **i**. Dot plot of the gene expression of domain-specific markers. The dot size represents the fraction of cells in a domain expressing the marker and the color intensity represents the average expression of the marker in that domain. **j.** Spatial expression for representative markers of the identified domains.

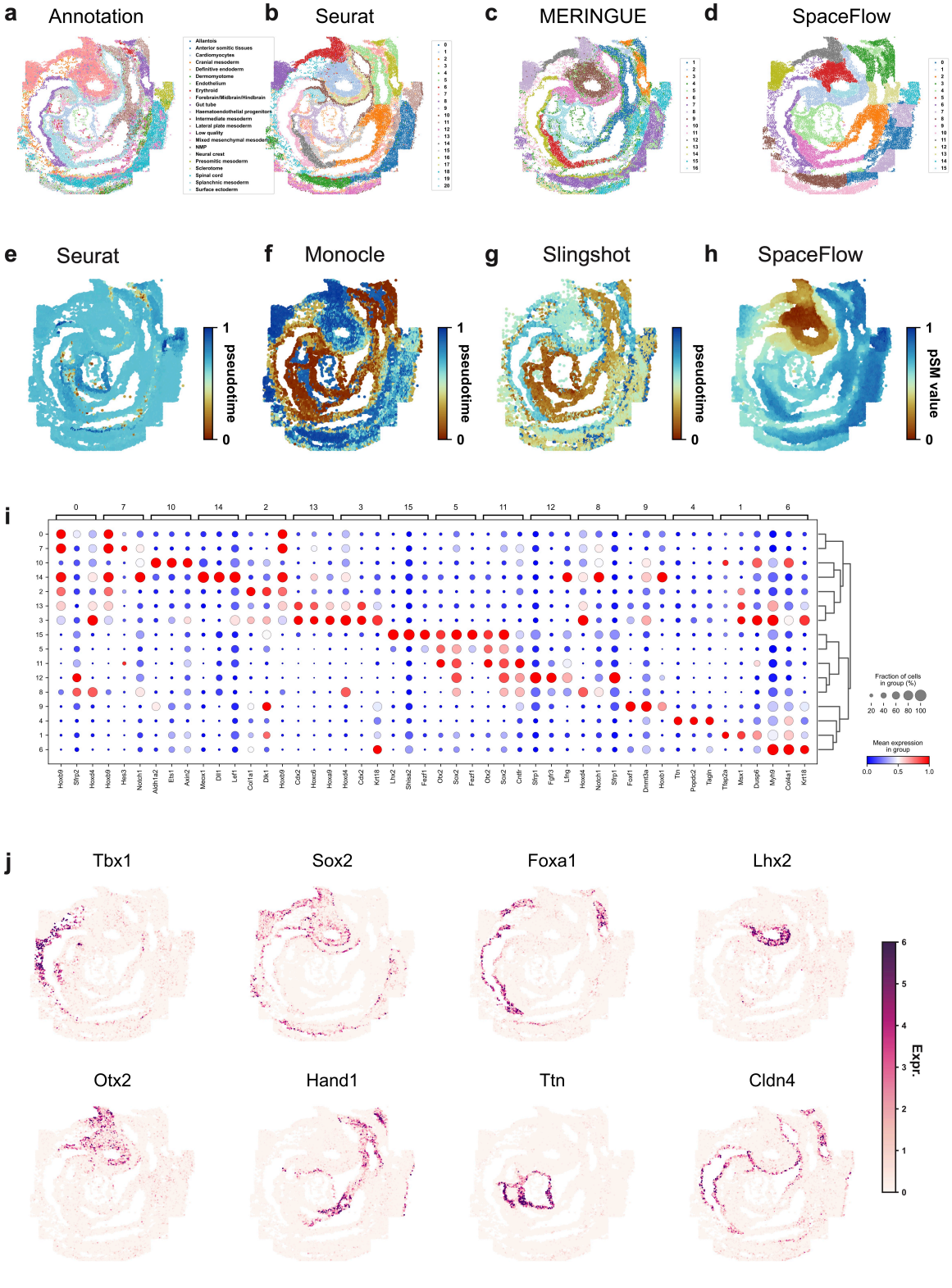
a
Annotation
Allantois
Anterior somitic tissues
Cardiomyocytes
Cranial mesoderm
Definitive endoderm
Dermomyotome
Endothelium
Erythroid
Forebrain/Midbrain/Hindbrain
Gut tube
Haematoendothelial progenitors
Intermediate mesoderm
Lateral plate mesoderm
Low quality
Mixed mesenchymal mesoderm
NMP
Neural crest
Presomitic mesoderm
Sclerotome
Spinal cord
Splanchnic mesoderm
Surface ectoderm
b
Seurat
c
MERINGUE
d
SpaceFlow
e
Seurat
f
Monocle
g
Slingshot
h
SpaceFlow
1
pseudotime
0
1
pseudotime
0
pseudotime
1
pSM value
0
i
0
7
10
14
2
13
3
15
5
11
12
8
9
4
1
6
Hoxb9
Sfrp2
Hoxd4
Hoxb9
Hes3
Notch1
Adh1a2
Ets1
Axin2
Mecr1
Dll1
Lef1
Col1a1
Dlk1
Hoxb9
Cdx2
Hoxc6
Hoxb9
Hoxd4
Cdx2
Krt18
Lhx2
Shisa2
Fezf1
Otx2
Sox2
Fezf1
Otx2
Sox2
Cntfr
Sfrp1
Fgf3
Lhx
Hoxd4
Notch1
Sfrp1
Foxf1
Dnmt3a
Hoxb1
Ttn
Popdc2
Tagln
Tfap2a
Mxi1
Dusp6
Myh9
Col4a1
Krt18
Fraction of cells in group (%)
20 40 60 80 100
Mean expression in group
0.0 0.5 1.0
j
Tbx1
Sox2
Foxa1
Lhx2
Otx2
Hand1
Ttn
Cldn4
Expr.
6
5
4
3
2
1
0

Supplementary Figure 5. SpaceFlow analysis on seqFISH mouse embryogenesis dataset [3]. a- Annotation **b-d**. Domain segmentations produced by Seurat (**b**), MERINGUE (**c**) and SpaceFlow (**d**). **e-h**. The spatial visualization of pseudotimes calculated by Seurat (**e**), Monocle (**f**), Slingshot (**g**), and the pSM generated by SpaceFlow (**h**). **i**. Dot plot of the gene expression of domain-specific markers. The dot size represents the fraction of cells in a domain expressing the marker and the color intensity represents the average expression of the marker in that domain. **j.** Spatial expression for representative markers of the identified domains.

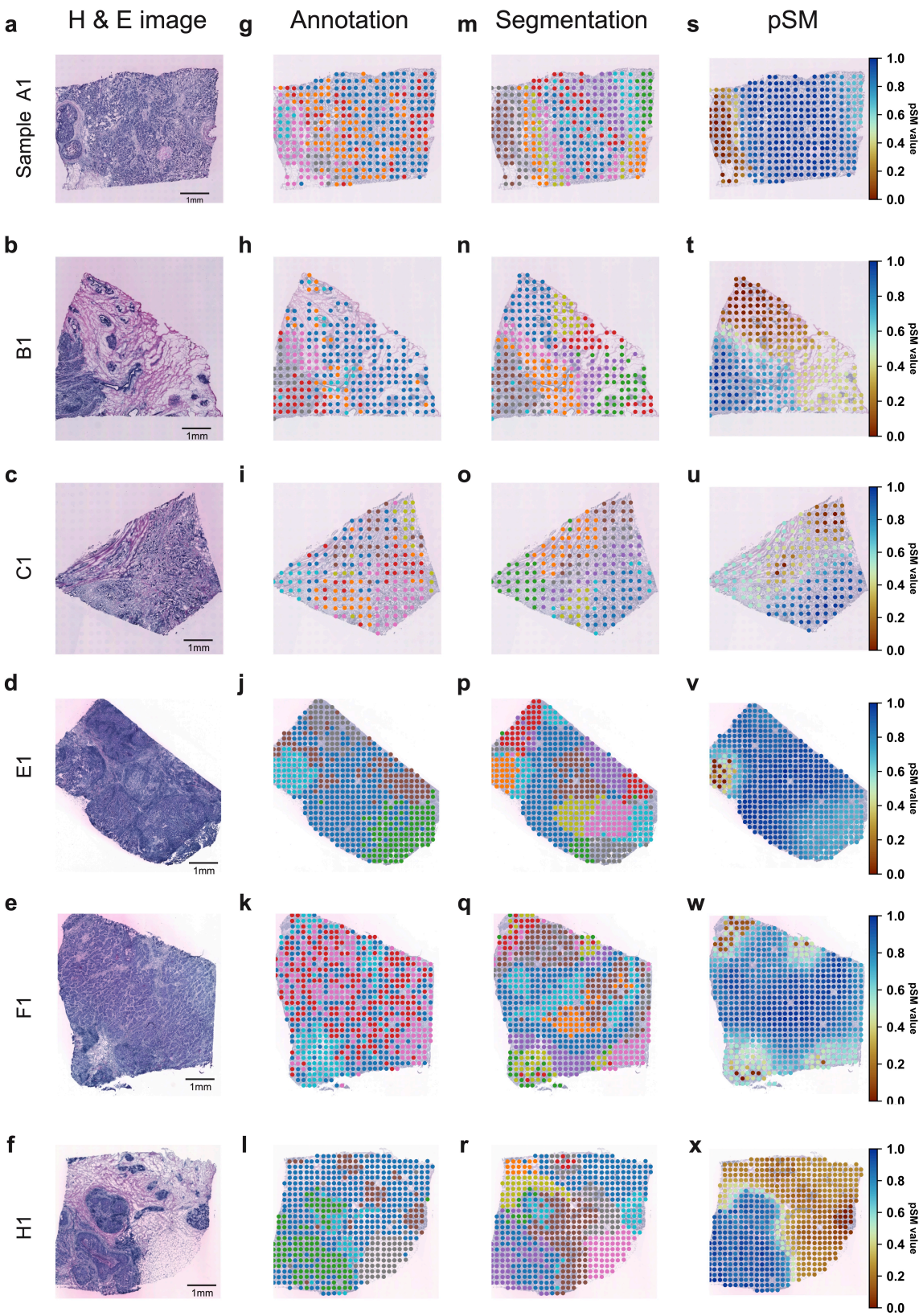
a
H & E image
g
Annotation
m
Segmentation
s
pSM
Sample A1
B1
C1
E1
F1
H1
b
h
n
t
c
i
o
u
d
j
p
v
e
k
q
w
f
l
r
x
1mm
pSM value
1.0
0.8
0.6
0.4
0.2
0.0

Supplementary Figure 6. Domain segmentation and pSM on six samples of Human Breast Cancer datasets [4]. a-f. H & E images of the six samples (Sample A1, B1, C1, E1, F1, H1, respectively). **g-l.** Annotations of the datasets given by the original paper. **m-r.** Domain segmentations of the datasets given by SpaceFlow. **s-x**. pSM of the datasets given by SpaceFlow.

Supplementary Tables

Supplementary Table 1. Functional Roles of Ligand Receptors showed cell-cell communications in human breast cancer progression

Ligand/Receptors	Function in Tumor Progression
COL1A1, COL1A2, COL6A1, COL6A2, COL6A3, COL4A2	As components of the extracellular matrix (ECM), and has been shown to promote invasion, metastasis, proliferation, tumorigenesis, death resistance of cancer cells, and regulate anti-tumor immunity, hypoxic condition. Cancer cells also can reversely reshape collagen to construct a positive feedback loop, which gradually encourages cancer progression.[5]
SDC1	Facilitate breast cancer metastasis.[6,7]
SDC4	The upregulation contributes to epithelial to mesenchymal transition (EMT) of cancer cells.[8]
CD44	The activation result in the activation of signaling pathways that induce cell proliferation and survival, regulate cytoskeletal changes, and encourage cellular motility. CD44 may also play roles in EMT and the adaptive plasticity of cancer cells.[9]
APP	Promote the migration and invasion of breast cancer cells by regulating the MAPK signaling pathway.[10]
CD74	Interact with CD44 and promote tumorigenesis and metastasis via RHOA-mediated cofilin phosphorylation in human breast cancer cells.[11]
MDK	A key player in cancer progression.[12]

Reference

1. Maynard, K. R. *et al.* Transcriptome-scale spatial gene expression in the human dorsolateral prefrontal cortex. *Nat. Neurosci.* **24**, 425–436 (2021).
2. Stickels, R. R. *et al.* Highly sensitive spatial transcriptomics at near-cellular resolution with Slide-seqV2. *Nat. Biotechnol.* **39**, 313–319 (2021).
3. Lohoff, T. *et al.* Integration of spatial and single-cell transcriptomic data elucidates mouse organogenesis. *Nat. Biotechnol.* **40**, 74–85 (2022).
4. Andersson, A. *et al.* Spatial deconvolution of HER2-positive breast cancer delineates tumor-associated cell type interactions. *Nat. Commun.* **12**, 6012 (2021).
5. Xu, S. *et al.* The role of collagen in cancer: from bench to bedside. *J. Transl. Med.* **17**, 309 (2019).
6. Chute, C. *et al.* Syndecan-1 induction in lung microenvironment supports the establishment of breast tumor metastases. *Breast Cancer Res.* **20**, (2018).
7. Sayyad, M. R. *et al.* Syndecan-1 facilitates breast cancer metastasis to the brain. *bioRxiv* (2019) doi:10.1101/565648.
8. Toba-Ichihashi, Y., Yamaoka, T., Ohmori, T. & Ohba, M. Up-regulation of Syndecan-4 contributes to TGF-β1-induced epithelial to mesenchymal transition in lung adenocarcinoma A549 cells. *Biochem. Biophys. Rep.* **5**, 1–7 (2016).
9. Chen, C., Zhao, S., Karnad, A. & Freeman, J. W. The biology and role of CD44 in cancer progression: therapeutic implications. *J. Hematol. Oncol.* **11**, (2018).
10. Wu, X., Chen, S. & Lu, C. Amyloid precursor protein promotes the migration and invasion of breast cancer cells by regulating the MAPK signaling pathway. *Int. J. Mol. Med.* **45**, 162–174 (2020).
11. Liu, Z. *et al.* CD74 interacts with CD44 and enhances tumorigenesis and metastasis via RHOA-mediated cofilin phosphorylation in human breast cancer cells. *Oncotarget* **7**, 68303–68313 (2016).
12. Filippou, P. S., Karagiannis, G. S. & Constantinidou, A. Midkine (MDK) growth factor: a key player in cancer progression and a promising therapeutic target. *Oncogene* **39**, 2040–2054 (2020).